Non-Orthogonal Narrowband Internet of Things: A Design for Saving Bandwidth and Doubling the Number of Connected Devices

Tongyang Xu, *Member, IEEE*, and Izzat Darwazeh, *Senior Member, IEEE*

***Abstract*—Narrowband Internet of Things (NB-IoT) is a low power wide area network (LPWAN) technique introduced in 3GPP release 13. The narrowband transmission scheme enables high capacity, wide coverage, and low power consumption communications. With the increasing demand for services over the air, wireless spectrum is becoming scarce and new techniques are required to boost the number of connected devices within a limited spectral resource to meet the service requirements. This paper provides a compressed signal waveform solution, termed fast-orthogonal frequency division multiplexing (Fast-OFDM), to double potentially the number of connected devices by compressing occupied bandwidth of each device without compromising data rate and bit error rate performance. Simulation is first evaluated for the Fast-OFDM with comparisons to single-carrier-frequency division multiple access (SC-FDMA). Results indicate the same performance for both systems in additive white Gaussian noise channel. Experimental measurements are also presented to show the bandwidth saving benefits of Fast-OFDM. It is shown that in a line-of-sight scenario, Fast-OFDM has similar performance as SC-FDMA but with 50% bandwidth saving. This research paves the way for extended coverage, enhanced capacity and improved data rate of NB-IoT in fifth generation new radio networks.**

***Index Terms*—Experiment, fifth generation (5G), Internet of Things (IoT), low power wide area network (LPWAN), machine to machine, machine-type communication (MTC), narrowband, narrowband IoT (NB-IoT), nonorthogonal, spectral efficiency, testbed, waveform.**

I. Introduction

INTERNET of Things (IoT) technologies are becoming increasingly popular and their ubiquity is bound to become a fact with large number of devices connected to enable machine to machine communication applications. There are wired and wireless connection approaches between different devices. For wired connections [1], fiber is widely used due to its reliability, high security, and high bandwidth; such characteristics make fiber the medium of choice in applications, such as critical-IoT [2]. Many of the sensors-based IoT applications require flexible deployment, with wireless technologies. Based on radio signal coverage, IoT wireless technologies are categorized into short range and wide area network (WAN) technologies [3]. The short range technologies include Zigbee, Wi-Fi, and Bluetooth. Their applications are largely limited to indoor use, such as in smart houses and smart building. The leading WAN technology, termed low power WAN (LPWAN), is for long range communication applications, such as remote monitoring and remote measurement.

For typical wireless signal transmission, the signal band is chosen to be wide in order to achieve high throughput. However, for IoT networks, narrow transmission band suffices for most applications, thus allowing a massive number of devices to be connected, even when the available spectrum is limited and further allows enhanced network capacity and extended devices coverage [1]. LPWAN applies narrow signal bandwidth in order to mitigate the significant path loss coming from long transmission range. LPWAN applications can either operate on unlicensed spectrum or licensed spectrum. The representative techniques for unlicensed applications are LoRa [4] and SigFox [5]. Both have information security challenges due to public sharing of their unlicensed spectral band. The spectrally licensed techniques overcome this challenge by reusing existing cellular networks, standardized by 3GPP. The representative technique is narrowband IoT (NB-IoT), [3], [6]–[10], which was first supported in 3GPP release 13 and it is foreseen in [11] that NB-IoT will be one of the technologies in 5G new radio (NR) networks. The signal is designed based on long term evolution (LTE) standard. Thus, it allows low-cost and fast deployment within existing physical infrastructure. In addition, since the signal is integrated within LTE signals, secure communications are guaranteed. In NB-IoT, the downlink employs orthogonal frequency division multiplexing (OFDM) while its uplink is single-carrier-frequency division multiple access (SC-FDMA) chosen for its reduced peak-to-average power ratio (PAPR).

NB-IoT provides wider coverage services for massively connected low data rate and low power consumption devices. The work in [3] has recently reported that NB-IoT can support up to 52547 devices per cell. As the demand for connected devices increases exponentially, the current capacity may not be sufficient for next generation networks. Therefore, increasing the connected devices within a cell is of importance.

Manuscript received February 2, 2018; revised March 21, 2018; accepted April 3, 2018. Date of publication April 9, 2018; date of current version June 8, 2018. This work was supported in part by the Engineering and Physical Sciences Research Council Impact Acceleration Discovery to Use Award (Grant reference: EP/R511638/1) and in part by the EU Funded 5G Exchange Innovation Project. *(Corresponding author: Tongyang Xu.)*

The authors are with the Department of Electronic and Electrical Engineering, University College London, London, WC1E 7JE, U.K. (e-mail: t.xu@ee.ucl.ac.uk; i.darwazeh@ucl.ac.uk).

Digital Object Identifier 10.1109/JIOT.2018.2825098

TABLE I
NB-IoT TESTBED COMPARISONS

Parameters/References	[8]	[12]	[13]	[14]	This Work
Developer	Zhejiang University	Virginia Tech	Keysight	Nutaq	UCL
Testbed	Tailored NB-IoT development Testbed	LTE-Cognitive Radio Network Testbed	E7515A UXM Wireless Test Set	Pico LTE	Software Defined NB-IoT Testbed
Scope	Academic research	Academic research	Academic research and industrial test	Academic research and industrial test	Academic research
Functionality	Commercial applications development	Co-existence of NB-IoT and Radar	Test and measurement	Test and measurement	Physical layer signal waveform optimization
User Defined Signal	No	No	No	No	Yes

This paper studies an approach for doubling the number of connected devices through using bandwidth compressed signal waveforms. Thus, spectral resource can be saved and reserved for extra devices. In this paper, a signal waveform termed Fast-OFDM [15]–[18], saving 50% of bandwidth, is theoretically and practically investigated for the NB-IoT applications. Simulation shows that Fast-OFDM and SC-FDMA achieve the same performance in additive white Gaussian noise (AWGN) channel. The theoretical predictions of the work presented here are verified experimentally. A practical software defined NB-IoT testbed is set up for this purpose with experimental data collected and practical results compared to those of simulations. There are other existing NB-IoT platforms being used as presented in Table I. The testbeds introduced in work [8], [12]–[14] implemented full functions of NB-IoT either for academic research or industrial test. However, their NB-IoT modules are fixed and designed based on the standard [19] and therefore maintaining the bandwidth and/or the number of connected devices. For research and development purposes, in some scenarios, novel signal waveforms have to be designed. Therefore, the NB-IoT module should be programmable. Our NB-IoT platform is software defined and can be used to test various signal formats, although the purpose of its use in this paper is to verify a newly proposed signal format, namely Fast-OFDM.

The advantages of using Fast-OFDM signals in NB-IoT scenarios are clearly demonstrated in this paper. To design the bandwidth compressed signal waveform, standard signal format may have to be slightly modified. Fortunately, the 3GPP release 14 [19] offers space to include new signal formats. There are several reserved modulation and coding scheme options in the standard; this gives room to implement non-standardized new signal formats. In this paper, we focus on an NB-IoT like deployment scenario in physical layer. The signal format we proposed follows typical NB-IoT standard signal but with minor modifications.

II. PRINCIPLE OF NB-IoT

There are three NB-IoT deployment modes: in-band, guard-band, and standalone [3]. The in-band deployment indicates that the NB-IoT signal can be integrated in existing LTE resource blocks. The guard-band deployment makes use of the guard band between adjacent LTE signal bands. The standalone scheme enables deployment in dedicated spectrum, such as global system for mobile communication. Each mode occupies a channel bandwidth of 200 kHz and a data

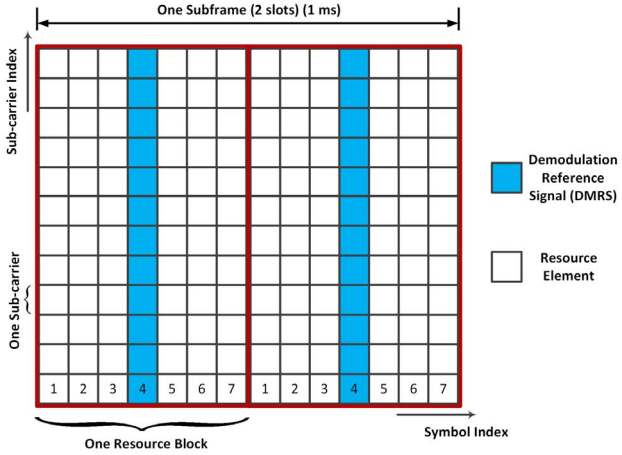

Fig. 1. NB-IoT uplink resource block definition and location of demodulation reference signals for a single antenna system.

bandwidth of 180 kHz. Both $\pi/2$-binary phase shift keying ($\pi/2$-BPSK) and quadrature phase-shift keying (QPSK) modulation schemes can be used and information modulated on 12 subcarriers with 15kHz sub-carrier spacing.

Work in [20] has studied the performance of spectrally efficient frequency division multiplexing (SEFDM) in a downlink IoT scenario. SEFDM [21]–[24] is a nonorthogonal signal waveform with its sub-carrier spacing equals α/T where α<1 is the bandwidth compression factor. Due to the self-created inter carrier interference (ICI), the receiver requires complicated signal processing, which inevitably consumes more power on each device. Notwithstanding, SEFDM is considered as a suitable signal waveform for 5G applications [25], [26]. Another specially efficient signal waveform, termed truncated OFDM, [27], could bring benefits to IoT applications via delivering data in a shorter time period. However, the introduced ISI would complicate the IoT device as well. In order to achieve ultra low power consumption, the design of each device should be as simple as possible. Therefore, any complicated signal processing should be within a base station or a central unit. Therefore, this paper is focused on the uplink design since most signal processing remains at the receiver.

The physical resource block mapping of uplink NB-IoT signals has been shown in [28] and in Fig. 1. The demodulation reference signal (DMRS), which is used for channel estimation, is different compared to the downlink one. In each slot, the fourth symbol, DMRS, carries pilot tones. There are 12 pilot tones in one slot while two groups of pilot symbols in

one subframe. This data and reference signal allocation will simplify the channel estimation and channel equalization.

Work in [29] studied uplink scheduling and link adaptation schemes without waveform optimization. This paper will adopt new waveforms, study its performance and show that the number of connected IoT devices could be doubled within the same 180 kHz bandwidth allocation.

III. Bandwidth Compressed Signal Waveform

The basic principle of bandwidth compression is to pack subcarriers nonorthogonally whilst maintaining the same data rate for each sub-carrier. Two benefits are introduced from the bandwidth compression. On one hand, noise power is reduced since the signal bandwidth is compressed. Thus, signal-to-noise ratio (SNR) is improved and communication coverage could be extended. On the other hand, bandwidth is saved and can be further reserved for other devices. Therefore, the number of connected devices may be increased.

A. Fast-OFDM

Fast-OFDM was first proposed in [15] as a wireless technique where it was shown to have similar performance to OFDM whilst saving 50% of bandwidth [16]–[18]. Such advantage encourages wide adoption of Fast-OFDM in optical systems [30] and more recently proposals for its use in visible light communication systems [31]. This multiplexing scheme packs subcarriers closer than a typical OFDM. Specifically, the sub-carrier spacing in Fast-OFDM is half of that in OFDM. However, the orthogonality property is still largely maintained at the cost that only 1-D modulation schemes can be employed. The Fast-OFDM signal is expressed as

$$x(t) = \sum_{k=0}^{N-1} X[k] e^{j2\pi \frac{k}{2T} t} \tag{1}$$

where $X[k]$ is 1-D modulation symbols (e.g., BPSK or m-ary amplitude shift keying (MASK) [32]) and N is the number of subcarriers. The sub-carrier spacing equals $(1/2T)$ and the center frequency for each sub-carrier is defined as $(k/2T)$. Considering two arbitrary subcarriers, hence, the orthogonal characteristic is verified by correlating two modulated symbols using the following equations:

$$\begin{aligned} \text{corr}(m,n) &= \frac{1}{T}\int_0^T X[m]X[n]\left(e^{j2\pi \frac{m}{2T}t}\right)\left(e^{j2\pi \frac{n}{2T}t}\right)^* dt \\ &= X[m]X[n]\{\text{sinc}[\pi(m-n)] \\ &\quad + j\cdot \frac{\pi(m-n)}{2}\cdot \text{sinc}^2\left[\frac{\pi(m-n)}{2}\right]\} \end{aligned} \tag{2}$$

where its real and imaginary parts are shown in (3) and (4), respectively,

$$\Re\{\text{corr}(m,n)\} = \begin{cases} X[m]X[n], & m = n \\ 0, & m \neq n \end{cases} \tag{3}$$

$$\Im\{\text{corr}(m,n)\} = \begin{cases} 0, & m = n \\ \frac{\pi(m-n)}{2}\cdot \text{sinc}^2\left[\frac{\pi(m-n)}{2}\right], & m \neq n \end{cases} \tag{4}$$

It is emphasized here that (3) and (4) are derived and valid provided that $X[m]$ and $X[n]$ are 1-D modulated symbols. The auto-correlation in (3) is not zero while the cross-correlation is zero indicating the real part satisfies the orthogonality requirement. However, this is not the case for the imaginary part as shown in (4) where its cross-correlation equals zero only when $m-n = 2\lambda$ where λ are integer values. In other words, the sub-carrier spacing should be a multiple of $(1/T)$ leading to the same spectral efficiency as OFDM. At the receiver, when real modulation symbols like BPSK or MASK are used, demodulation using complex subcarriers with frequency separation of $(1/2T)$, the real part is easily recovered but with added distortion appearing as imaginary terms. Therefore, the real part of the symbol, which carries information can be transmitted with no distortion. Conversely, when complex modulation symbols are used, demodulation at the receiver will result in distortion of both the real and imaginary part of the signal. As such, a proper signal recovery will require complex detection techniques [33]. To sum up, this technique can achieve the same performance as OFDM with 1-D modulation scheme like BPSK or MASK. With the enlargement of modulation levels, performance is degraded significantly. Therefore, by transmitting the same amount of data, the spectral efficiency is doubled since 50% of bandwidth is saved. In terms of system design, the Fast-OFDM can directly employ inverse fast Fourier transform (IFFT) and fast Fourier transform (FFT) at the transmitter and the receiver, respectively. Other techniques for Fast-OFDM signal generation have been considered and these include the elegant method of using inverse discrete cosine transform (IDCT) in [30] for optical systems, where double-side band Fast-OFDM are generated and where these can be modified into single-side band Fast-OFDM using Hilbert transform. In this paper, we choose the use of IFFT signal generation, initially proposed for SEFDM [23], [34], to maintain compatibility with LTE/NB-IoT standards.

The graphical explanation of Fast-OFDM is shown in Fig. 2 where two spectra are compared. The first one is a typical OFDM spectrum, which shows orthogonally packed subcarriers. The second one is Fast-OFDM with the same sub-carrier bandwidth and the same number of subcarriers but with 50% closer sub-carrier spacing. Therefore, the bandwidth is saved by 50%. The saved bandwidth could be reserved for extra devices.

B. Signal Processing

This paper represented here is focused on the uplink channel and all the signal processing, such as channel estimation, channel equalization, timing synchronization, phase compensation, and signal detection are within base station. NB-IoT devices are only responsible for generating SC-FDMA/Fast-OFDM signals and sending signals to a base station or a central unit. Thus, low power consumption of each IoT device is guaranteed.

Multipath propagation is a challenging issue because both amplitude and phase can change at the same time. Although work in [35] proposed specially designed symmetric extension-based guard interval and one-tap equalizer for the channel equalization, the IDCT-based signal processing is not compatible with existing LTE/NB-IoT standards. In order

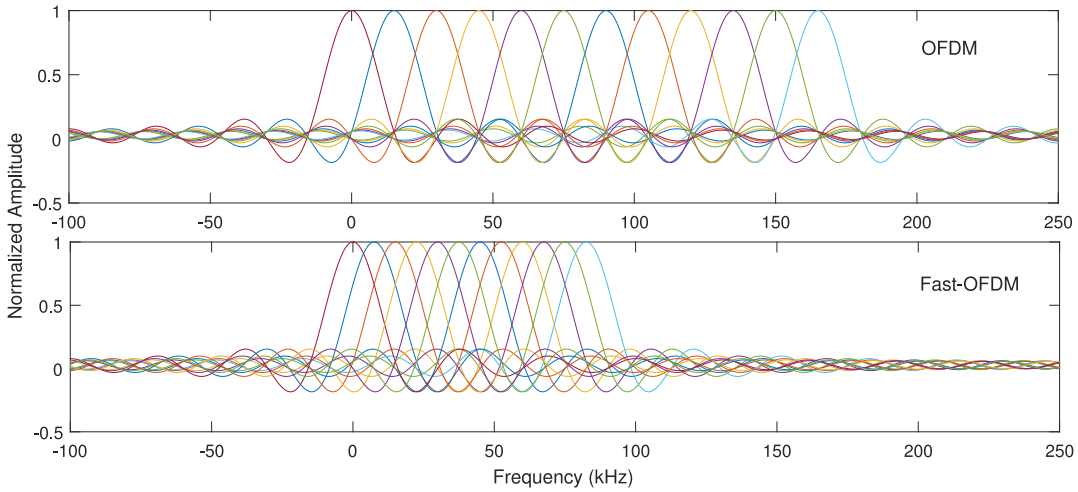

Fig. 2. Sub-carrier allocation schemes for different multicarrier signal waveforms.

to maintain the compatibility, we employed the typical cyclic prefix (CP) following the standards and the frequency-domain least square (LS) method [36], [37]. IoT devices are usually deployed in a static or semi-static channel environment. Thus, unlike LTE signals, NB-IoT signals would experience slow time-changing or time-invariant channels. Therefore, in this paper, the channel is assumed static within one resource block and one DMRS (illustrated in Fig. 1), can estimate the channel and equalize the channel for the symbols within one resource block. In order to get more accurate channel state information (CSI), two channel frequency responses extracted from two block-type pilot symbols within one subframe can be averaged. Thus, the averaged CSI can be used to equalize the data symbols within one subframe.

In order to demodulate and recover signals properly, the exact starting point of received data stream has to be located, which means correct symbol timing synchronization is required. The self-created ICI from Fast-OFDM will affect timing synchronization accuracy. The work in [38] proposed a two-stage timing synchronization approach for Fast-OFDM. However, the complexity makes such estimation unsuitable for IoT scenarios. In this paper, for simplicity we adopt Schmidl and Cox timing synchronization sequence [39], which has proven to be efficacious in previous experiments with SEFDM [23], [40]. The basic principle is to send two identical sequences and their correlation is calculated at the receiver. The correlation peak indicates the actual beginning of a data stream.

Phase distortions from local oscillators, imperfect timing synchronization and unmatched sampling clocks also exist in realistic systems. Imperfect matching of transmitter and receiver local oscillators leads to fixed phase offset, which can be cancelled using the LS method [37]. The timing synchronization is affected by noise and interference, which result in sub-carrier index dependent phase offset [37]. The phase offset from unmatched sampling clocks is usually small, and it is often treated as a part of imperfect timing synchronization. All the aforementioned offsets can be compensated jointly using the LS channel compensation algorithm. It should be noted that the typical LS method for Fast-OFDM will introduce equalization errors because of the ICI. In a realistic NB-IoT scenario, Turbo coding [6] is employed. Due to its powerful error correction capability, the equalization errors can be mitigated.

IV. Simulation Evaluation

In this paper, $\pi/2$-BPSK modulation scheme is employed for SC-FDMA following the LTE release 14 standard [19]. This modulation scheme is derived based on typical BPSK via rotating every other symbol by $\pi/2$. It has the same bit error rate (BER) performance as the typical BPSK, but with additional benefits, such as smaller envelope variation [41], which leads to reduced PAPR. Therefore, it is preferred in NB-IoT scenario. For Fast-OFDM, as discussed in Section III-A, only 1-D modulation schemes are viable. The special constellation pattern introduced by $\pi/2$-BPSK, illustrated in [41], is similar to a 2-D modulation format. Thus, $\pi/2$-BPSK is infeasible and BPSK is preferred to Fast-OFDM. For higher order modulation formats, supported by NB-IoT, such as QPSK is not achievable for Fast-OFDM. However, an evolved nonorthogonal signal waveform, termed SEFDM, [21], [23], can use modulation formats up to 16QAM at the expense of increased complexity.

A. Constellation Patterns

The constellation diagrams of SC-FDMA and Fast-OFDM are shown in Fig. 3 where three constellation patterns are illustrated. For the Fast-OFDM signal as discussed in Section III-A, the real part of the signal is not affected by any interference. Thus, the demodulated constellation in Fig. 3(a) shows vertically aligned points. However, its imaginary part is significantly interfered and the length of the vertical line determines the interference level. Fig. 3(b) shows the constellation performance of Fast-OFDM signals in AWGN channel. The constellation points distribute as a vertical line as well. Meanwhile, its points are scattered horizontally, which indicates distortions to the real part signals. For the SC-FDMA

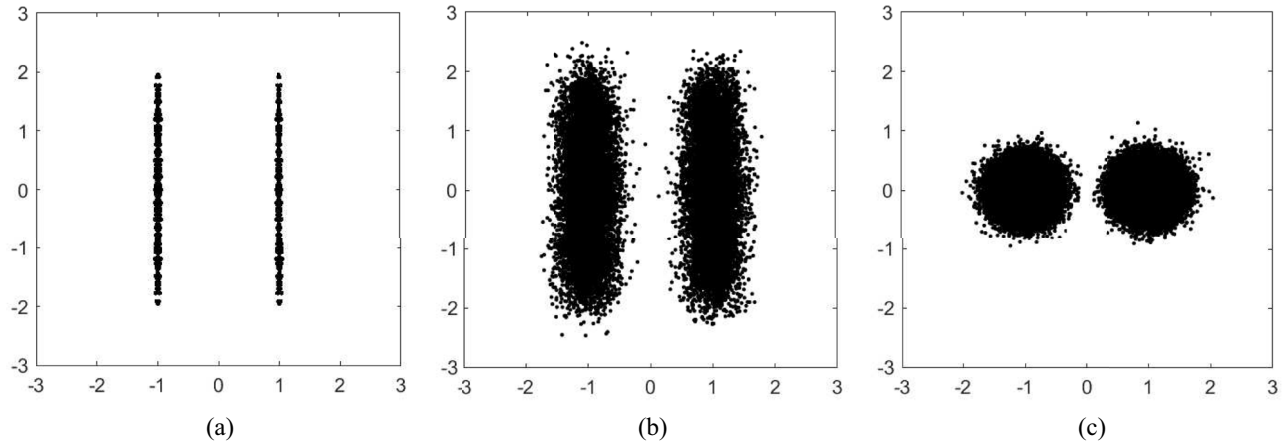

Fig. 3. BPSK constellation demonstrations for Fast-OFDM and SC-FDMA. (a) Ideal Fast-OFDM. (b) Fast-OFDM in AWGN channel at $E_b/N_o = 10$ dB. (c) SC-FDMA in AWGN channel at $E_b/N_o = 10$ dB.

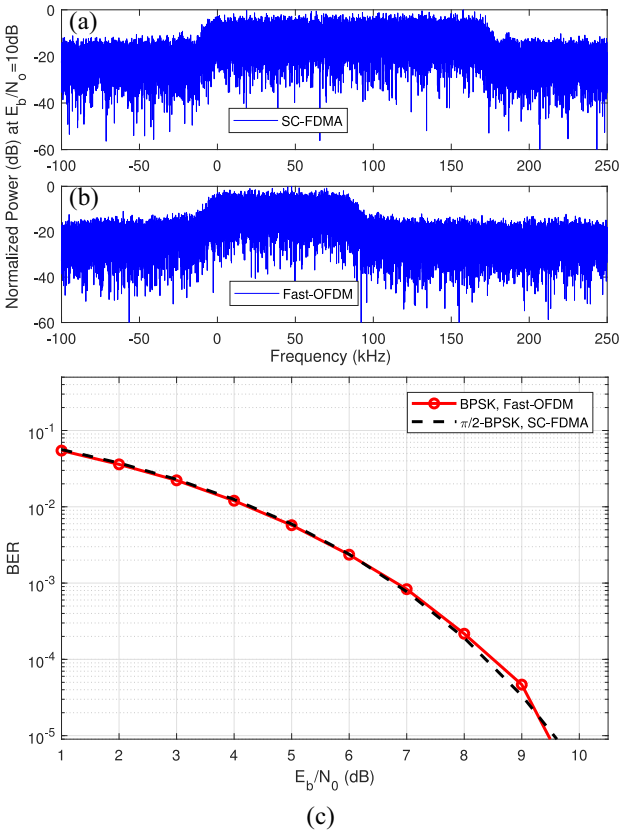

Fig. 4. Spectra and performance comparisons of BPSK modulated Fast-OFDM signal and $\pi/2$-BPSK modulated SC-FDMA signal in the NB-IoT scenario. (a) Spectrum of SC-FDMA. (b) Spectrum of Fast-OFDM. (c) BER performance of the two systems.

signals as shown in Fig. 3(c), with E_b/N_o=10 dB AWGN noise the two constellation points are scattered equally in vertical and horizontal directions.

B. Performance in AWGN Channel

The spectra of SC-FDMA/Fast-OFDM and their BER performance in AWGN channel are shown in Fig. 4. The bandwidth of the SC-FDMA signal is 180 kHz while with 50% bandwidth compression of Fast-OFDM, the bandwidth is compressed to 90 kHz. It should be noted that the overall data rate remains the same for both systems. BER performance is studied for both uncoded SC-FDMA and Fast-OFDM signals in Fig. 4(c). For the two systems, matched filter detectors are employed to recover signals at the receiver. It is clearly seen that both systems have the same BER performance.

V. Implementation and Verification

In this section, the bandwidth compressed NB-IoT system is implemented on the Aeroflex PCI extensions for instrumentation (PXI) software defined IoT platform [42]–[44]. The testbed used in this experiment is in Fig. 5, where the top left is the general block diagram of the system. The real experimental setup is shown on the bottom left in Fig. 5 where one PXI software defined IoT platform, a Spirent channel emulator VR5 [45], a signal splitter and a spectrum analyzer are connected.

The detailed experiment operation block diagram is illustrated in Fig. 6. The main benefit of this testbed is that the entire NB-IoT system can be jointly realized in software and hardware. MATLAB is the software tool that implements part of the functions aligning with hardware integrated in the PXI platform. The software defined IoT platform works as a signal transceiver, which has functions, such as signal generation, signal reception, digital-to-analogue conversion (DAC)/analog-to-digital conversion (ADC) and up/down-conversions. It is the main platform in this experiment.

The digital bit stream is first generated in transmitter software environment. LTE standardized Turbo coding [6] is applied in this paper to mitigate the channel and noise effects. The data is Turbo encoded using a code rate $R_{\text{code}} = 1/3$. The code used is a (13,15) code of memory 3 with feedforward polynomial $G_1(D) = 1 + D + D^3$ and feedback polynomial $G_2(D) = 1 + D + D^2 + D^3$. The encoded bit stream is then mapped to either BPSK symbols for Fast-OFDM or $\pi/2$-BPSK symbols for SC-FDMA. The serial symbol stream is converted to parallel streams. Then, block-type pilot symbols are added in the middle of each resource block, as

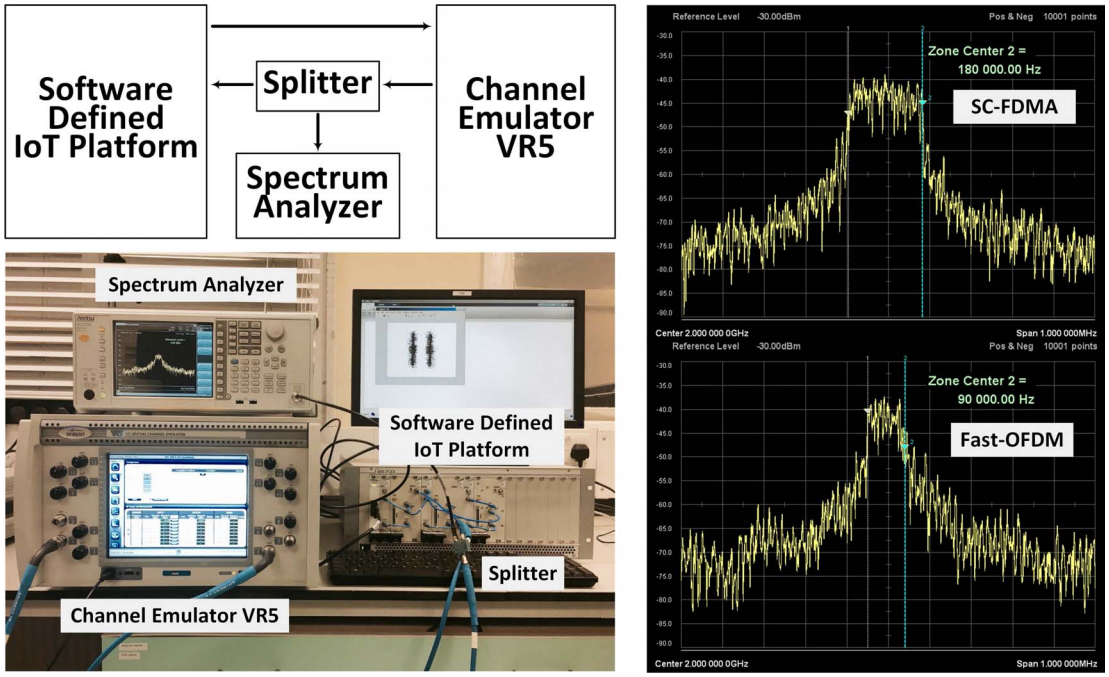

Fig. 5. Implemented software defined NB-IoT experimental testbed with measured spectra for SC-FDMA and Fast-OFDM signals.

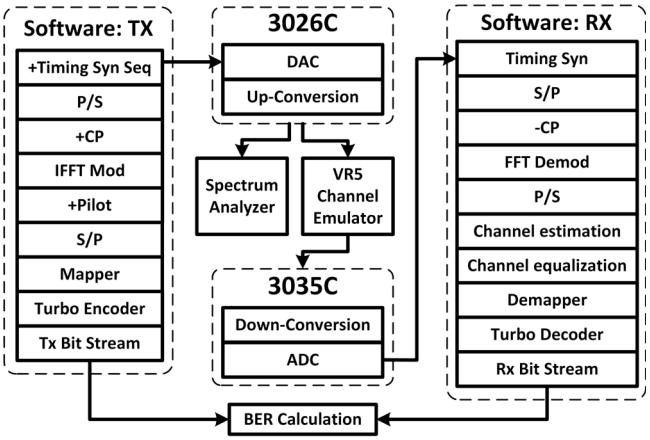

Fig. 6. Block diagram of step-by-step operations for the nonorthogonal NB-IoT experimental testbed.

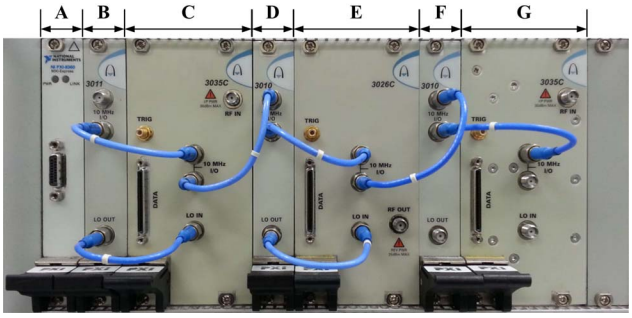

Fig. 7. Cable connections on the front panel of PXI.

illustrated in Fig. 1. After Fast-OFDM or SC-FDMA IFFT modulation, CP is added for channel compensation purpose. Afterward, the parallel streams are converted to a serial stream with the timing sequence added at the beginning. Thus, the digital signal is generated at the transmitter.

The analogue signal processing is integrated in the PXI chassis. Two crucial modules inside the PXI are 3026C RF signal generator and 3035C RF signal digitizer. The carrier frequency ranges from 100 kHz to 6 GHz in both modules. Up to 90 MHz RF modulation bandwidth and 512 MHz sampling rate are supported. The fixed-point resolution is 32 bit sample word consisting of 14 bit I data, 14 bit Q data, and 4 bit marker data. The detailed information of the front panel of the PXI chassis is provided in Fig. 7, where the cable connections of different modules on the front panel of PXI are illustrated. The module labeled A is the power and digital signal provider. Digital signals from a PC will be delivered to this module via the serial interference. Modules B, D, F are clock boards, which provide 10 MHz reference signal and local oscillator (LO) signal to the 3026C RF signal generator and 3035C RF digitizer. Module C, G are the 3035C RF signal receivers (digitizers) and module E is the 3026C RF signal generator. Although there are three separate clock boards, all the modules are synchronized by the 10 MHz reference signal from module B attempting to establish a frequency-offset-free condition.

The analogue signal is generated after the DAC and up-conversion within the 3026C RF signal generator and then sent to the Spirent channel emulator VR5 [45] for channel impairment testing. The channel emulator can emulate various wireless channels including line-of-sight (LOS) and non-LOS (NLOS) channels. NLOS channels bring frequency selective distortions to signals. The narrower signal bandwidth of Fast-OFDM can avoid poor quality channels and therefore, depending on the channel, it could bring higher SNR and better

TABLE II
EXPERIMENT SPECIFICATIONS

Parameters	SC-FDMA	Fast-OFDM
Occupied Channel Bandwidth (kHz)	180	90
Bit rate (kbit/s)	180	180
Bit rate per sub-carrier (kbit/s)	15	15
Sub-carrier bandwidth (kHz)	15	15
Sub-carrier spacing (kHz)	15	7.5
Sampling rate (MHz)	1.92	1.92
FFT size	128	128
Number of cyclic prefix samples	10	10
Number of guard band sub-carriers	58	58
Number of data sub-carriers	12	12
Modulation scheme	$\pi/2$-BPSK	BPSK

performance. This will result in unfair comparisons with SC-FDMA whose wide bandwidth may experience poor channel conditions. Therefore, in this experiment, for fair comparisons, we only studied LOS channel models.

The output from the VR5 is the signal that experiences path loss and noise distortion. The first copy of the signal is delivered back to the software defined IoT platform, 3035C RF signal digitizer, for down-conversion and ADC. Its second copy is diverted via the splitter to the spectrum analyzer. Two measured spectra are saved and shown on the right side in Fig. 5. The first spectrum is SC-FDMA, which occupies bandwidth of 180 kHz and the second one is Fast-OFDM, which occupies bandwidth of 90 kHz. Thus, the benefit of saving half bandwidth is verified by the spectrum analyzer.

The digital signal after 3035C RF signal digitizer is timing synchronized using the Schmidl and Cox algorithm [39]. The calibrated signal is converted to parallel streams. The CP is removed and each of the parallel streams are FFT demodulated. The demodulated symbol streams are converted back to a serial symbol stream for channel estimation and equalization. The equalized symbols are demapped back to bit streams according to the used modulation schemes. After Turbo decoding, the receiver bit stream is obtained. The BER is calculated by comparing the transmitter bit and receiver bit streams.

The experimental SC-FDMA/Fast-OFDM signals are generated based on the system specifications presented in Table II. Due to limitations of the testbed, the maximum transmit power is -16 dBm, which would limit the signal transmission distance. The noise power at the receiver is set to -70 dBm with receiver bandwidth of 1 MHz and AWGN bandwidth of 1.25 MHz. In the experiment, shown in Table III, the signal receive power is changed flexibly to emulate the path loss and transmission distance. Thus, knowing the noise power (see Table III), the receiver SNR can easily be calculated.

Based on the system parameters in the experiment, path loss versus transmission distance and SNR versus transmission distance are plotted together in Fig. 8. As mentioned previously, due to the limited transmit power from the testbed, the maximum achievable path loss limits the transmission distance to approximately 23 m. With a power amplifier, the enhanced signal could be transmitted further. In Fig. 8, it is clearly seen that with the increase of transmission distance, SNR drops nonlinearly. Meanwhile, the path loss is increased nonlinearly

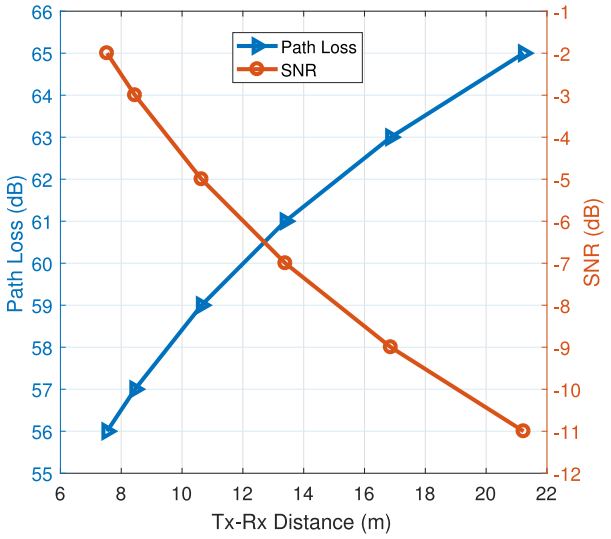

Fig. 8. Path loss and SNR performance versus transmitter and receiver distance.

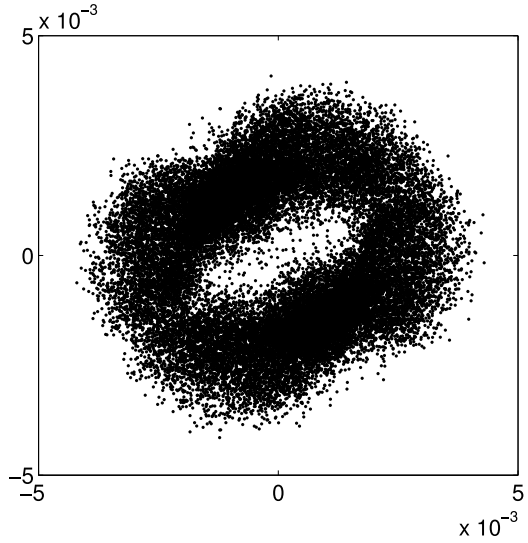

Fig. 9. Experimental BPSK constellation demonstrations for Fast-OFDM before equalization.

with the increase of transmission distance. This figure would give us a direction of designing NB-IoT devices.

Two constellation patterns are extracted from the testbed when the receiver power is -72 dBm, noise power is -70 dBm. Constellation is a criteria to verify the quality of the testbed and its different patterns indicate the potential issues on the platform. Figs. 9 and 10 present two constellation results collected from the practical testbed before and after signal equalization, respectively.

There are some conclusions derived from Fig. 9. First, the constellation rotates by a fixed degree, which may indicates the fixed phase offset from the LO. Second, the constellation has a tendency to rotate but not in a circle. It can be inferred that the signal is not affected by time dependent phase offset but suffers sub-carrier dependent phase offset. Therefore, frequency offset does not exist since it introduces time dependent

TABLE III
EXPERIMENTAL TRANSMISSION AND RECEPTION POWER AND CHANNEL INFORMATION

Tx Power(dBm)	Rx Power(dBm)	Path Loss(dB)	Noise Power(dBm)	SNR(dB)
-16	-81	65	-70	-11
-16	-79	63	-70	-9
-16	-77	61	-70	-7
-16	-75	59	-70	-5
-16	-73	57	-70	-3
-16	-72	56	-70	-2

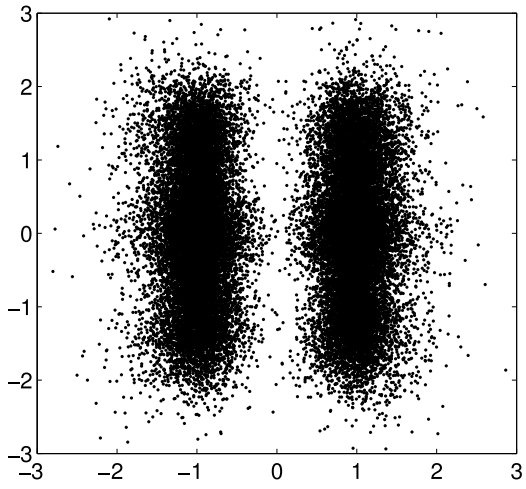

Fig. 10. Experimental BPSK constellation demonstrations for Fast-OFDM after equalization.

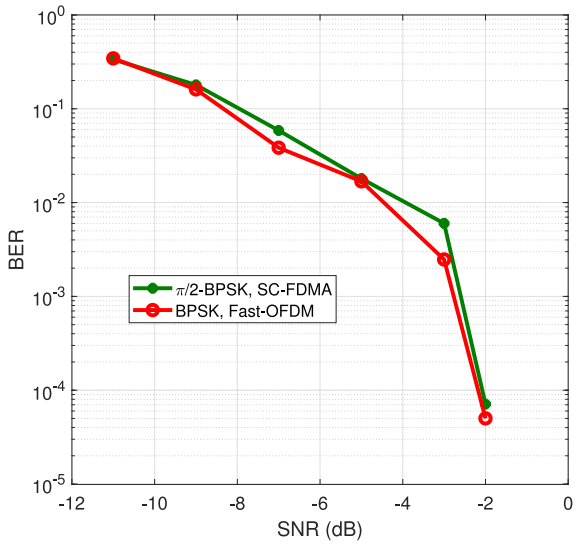

Fig. 11. Experimental BER performance comparison over a fixed noise bandwidth of 1.25 MHz.

phase offset. The testbed may have imperfect timing synchronization and unmatched sampling clock problems. Both factors can cause the sub-carrier dependent phase offset. One solution to verify the possible factors from the testbed is to do channel estimation and equalization on the rotated signal. The compensated constellation, shown in Fig. 10, is very similar to the simulation results in Fig. 3(b), where two vertical lines are observed. This result verifies the assumption since the frequency-domain LS channel compensation method cannot compensate the time dependent phase offset. All sub-carrier dependent phase offsets are removed. There are some scattering points around the two vertical lines. This could be caused by noise, which affects the channel estimation and equalization accuracy.

In this practical experiment, LOS channel scenario is considered, which assumes the channel response is almost flat, similar to the one in Fig. 4(a) and (b). Fig. 11 shows measurement results collected from the testbed and plotted as BER versus SNR for the Fast-OFDM and SC-FDMA systems with standard Turbo coding [6]. BER is calculated and SNR is derived based on the measurements in Table III. The measurements in the figure show that the performance of both systems is similar when the same testbed conditions are applied. It is worth noting that the same conclusion was predicted in simulations of both systems, of results presented in Fig. 4, showing BER versus E_b/N_0, where the same error rates were predicted for the two systems operating in a simple AWGN environment and with no coding. The simulation results shown in Fig. 4 assume AWGN channel while other distortion factors are not considered in this paper for simplicity. However, in the practical experiment, realistic distortions, such as imperfect channel estimation/equalization, imperfect timing synchronization, unmatched sampling clock, and LO phase offset exist. These factors will affect signal recovery.

VI. CONCLUSION

One challenge for LPWAN is to support a large number of devices within a limited spectral resource. NB-IoT can cope with this challenge by using narrowband signals. Thus, massively connected IoT devices can be aggregated with extra benefits, such as improved SNR and extended coverage. However, with the increasing demand for IoT services, more devices have to be connected. The limited spectral resource limits the total connected devices. This paper provides an efficient solution, which could double the number of connected devices, by using a bandwidth compressed signal waveform. First, this paper introduces basic principle of NB-IoT and followed by the description of the bandwidth compressed signal waveform Fast-OFDM. Then, we analytically studied the performance of the Fast-OFDM in terms of its constellation patterns and in AWGN channel. Simulation results show the same performance for both SC-FDMA and Fast-OFDM systems in AWGN channel. Finally, we reported experimental tests of the bandwidth compressed narrowband signal in a practical testbed in an LOS scenario. Experimental results verified the simulation conclusion that Fast-OFDM achieves

the same performance as SC-FDMA, but with twice spectral efficiency. This paper is focused on a new NB-IoT signal waveform design. Thus, the software defined NB-IoT testbed used here is aimed to modify physical layer with no support from media access control (MAC) and higher layers. However, in order to realize optimizing functions, such as scheduling and link adaptation, MAC layer feedback control information is required. Therefore, with higher layer protocols assistance, this paper could further lead to new research directions in extending coverage; enhancing capacity and improving data rates for 5G NR NB-IoT networks.

REFERENCES

[1] W. Yang *et al.*, "Narrowband wireless access for low-power massive Internet of Things: A bandwidth perspective," *IEEE Wireless Commun.*, vol. 24, no. 3, pp. 138–145, Jun. 2017.

[2] P. Schulz *et al.*, "Latency critical IoT applications in 5G: Perspective on the design of radio interface and network architecture," *IEEE Commun. Mag.*, vol. 55, no. 2, pp. 70–78, Feb. 2017.

[3] M. Chen, Y. Miao, Y. Hao, and K. Hwang, "Narrow band Internet of Things," *IEEE Access*, vol. 5, pp. 20557–20577, 2017.

[4] N. Sornin, M. Luis, T. Eirich, T. Kramp, and O. Hersent, "LoRaWAN specification, version 1.0," Tech. Document, LoRa Alliance, Jan. 2015.

[5] SigFox. *SigFox*. Accessed: Apr. 2018. [Online]. Available: https://www.sigfox.com

[6] "Feasibility study for further advancements for E-UTRA (LTE-advanced), rel. 13," 3GPP, Sophia Antipolis, France, Rep. 3GPP TR 36.912 v.13.0.0, Dec. 2015.

[7] Y. Miao, W. Li, D. Tian, M. S. Hossain, and M. F. Alhamid, "Narrow band Internet of Things: Simulation and modelling," *IEEE Internet Things J.*, to be published.

[8] J. Chen *et al.*, "Narrowband Internet of Things: Implementations and applications," *IEEE Internet Things J.*, vol. 4, no. 6, pp. 2309–2314, Dec. 2017.

[9] Y.-P. E. Wang *et al.*, "A primer on 3GPP narrowband Internet of Things," *IEEE Commun. Mag.*, vol. 55, no. 3, pp. 117–123, Mar. 2017.

[10] R. Ratasuk, N. Mangalvedhe, Y. Zhang, M. Robert, and J.-P. Koskinen, "Overview of narrowband IoT in LTE rel-13," in *Proc. IEEE Conf. Stand. Commun. Netw. (CSCN)*, Berlin, Germany, Oct./Nov. 2016, pp. 1–7.

[11] G. A. Akpakwu, B. J. Silva, G. P. Hancke, and A. M. Abu-Mahfouz, "A survey on 5G networks for the Internet of Things: Communication technologies and challenges," *IEEE Access*, vol. 6, pp. 3619–3647, 2018.

[12] S. Bhattarai, P. R. Vaka, and J.-M. Park, "Co-existence of NB-IoT and radar in shared spectrum: An experimental study," in *Proc. IEEE Glob. Commun. Conf. (GLOBECOM)*, Singapore, Dec. 2017, pp. 1–6.

[13] Keysight. *E7515A UXM Wireless Test Set*. Accessed: Apr. 2018. [Online]. Available: https://www.keysight.com/en/pd-2372474-pn-E7515A

[14] Nutaq. *Pico LTE—eNodeB and EPC in a Box for Test & Measurement*. [Online]. Available: https://www.nutaq.com/lte-enodeb-in-a-box

[15] M. R. D. Rodrigues and I. Darwazeh, "Fast OFDM: A proposal for doubling the data rate of OFDM schemes," in *Proc. Int. Conf. Telecommun.*, vol. 3. Beijing, China, 2002, pp. 484–487.

[16] K. Li, "Fast orthogonal frequency division multiplexing (Fast-OFDM) for wireless communications," Ph.D. dissertation, Dept. Electron. Elect. Eng., Univ. College London, London, U.K., 2008.

[17] D. Karampatsis, "Modelling and performances assessment of OFDM and fast-OFDM wireless communication systems," Ph.D. dissertation, Dept. Electron. Elect. Eng., Univ. College London, London, U.K., Aug. 2004.

[18] D. Karampatsis and I. Darwazeh, "Performance comparison of OFDM and FOFDM communication systems in typical GSM multipath environments," in *Proc. London Commun. Symp.*, London, U.K., 2003, pp. 360–372.

[19] *LTE; Evolved Universal Terrestrial Radio Access (E-UTRA); Physical Layer Procedures, Rel. 14*, 3GPP Standard TS 36.213 v.14.2.0, Apr. 2017.

[20] M. Jia, Z. Yin, Q. Guo, G. Liu, and X. Gu, "Downlink design for spectrum efficient IoT network," *IEEE Internet Things J.*, to be published.

[21] M. R. D. Rodrigues and I. Darwazeh, "A spectrally efficient frequency division multiplexing based communications system," in *Proc. 8th Int. OFDM Workshop*, Hamburg, Germany, 2003, pp. 48–49.

[22] T. Xu, R. C. Grammenos, F. Marvasti, and I. Darwazeh, "An improved fixed sphere decoder employing soft decision for the detection of non-orthogonal signals," *IEEE Commun. Lett.*, vol. 17, no. 10, pp. 1964–1967, Oct. 2013.

[23] T. Xu and I. Darwazeh, "Transmission experiment of bandwidth compressed carrier aggregation in a realistic fading channel," *IEEE Trans. Veh. Technol.*, vol. 66, no. 5, pp. 4087–4097, May 2017.

[24] H. Ghannam and I. Darwazeh, "SEFDM over satellite systems with advanced interference cancellation," *IET Commun.*, vol. 12, no. 1, pp. 59–66, Jan. 2018.

[25] W. Xiang, K. Zheng, and X. Shen, *Key Enabling Technologies for 5G Mobile Communications*. Cham, Switzerland: Springer, 2016.

[26] F.-L. Luo and C. Zhang, *Signal Processing for 5G: Algorithms and Implementations*. Chichester, U.K.: Wiley, 2016.

[27] W. Ozan, K. Jamieson, and I. Darwazeh, "Truncating and oversampling OFDM signals in white Gaussian noise channels," in *Proc. 10th Int. Symp. Commun. Syst. Netw. Digit. Signal Process. (CSNDSP)*, Prague, Czech Republic, Jul. 2016, pp. 1–6.

[28] Y. D. Beyene, R. Jantti, K. Ruttik, and S. Iraji, "On the performance of narrow-band Internet of Things (NB-IoT)," in *Proc. IEEE Wireless Commun. Netw. Conf. (WCNC)*, San Francisco, CA, USA, Mar. 2017, pp. 1–6.

[29] C. Yu, L. Yu, Y. Wu, Y. He, and Q. Lu, "Uplink scheduling and link adaptation for narrowband Internet of Things systems," *IEEE Access*, vol. 5, pp. 1724–1734, 2017.

[30] J. Zhao and A. D. Ellis, "Discrete-Fourier transform based implementation for optical fast OFDM," in *Proc. 36th Eur. Conf. Exhibit. Opt. Commun. (ECOC)*, Torino, Italy, Sep. 2010, pp. 1–3.

[31] P. Haigh and I. Darwazeh, "Visible light communications: Fast-orthogonal frequency division multiplexing in highly bandlimited conditions," in *Proc. IEEE/CIC Int. Conf. Commun. China (ICCC)*, 2017, pp. 1–8.

[32] F. Xiong, "M-ary amplitude shift keying OFDM system," *IEEE Trans. Commun.*, vol. 51, no. 10, pp. 1638–1642, Oct. 2003.

[33] I. Kanaras, A. Chorti, M. R. D. Rodrigues, and I. Darwazeh, "A combined MMSE-ML detection for a spectrally efficient non orthogonal FDM signal," in *Proc. 5th Int. Conf. Broadband Commun. Netw. Syst. (BROADNETS)*, London, U.K., Sep. 2008, pp. 421–425.

[34] P. N. Whatmough, M. R. Perrett, S. Isam, and I. Darwazeh, "VLSI architecture for a reconfigurable spectrally efficient FDM baseband transmitter," *IEEE Trans. Circuits Syst. I, Reg. Papers*, vol. 59, no. 5, pp. 1107–1118, May 2012.

[35] J. Zhao and A. D. Ellis, "Channel estimation and compensation in chromatic dispersion limited optical fast OFDM systems," in *Proc. 8th Int. Symp. Commun. Syst. Netw. Digit. Signal Process. (CSNDSP)*, Poznań, Poland, Jul. 2012, pp. 1–4.

[36] Y. Liu, Z. Tan, H. Hu, L. J. Cimini, and G. Y. Li, "Channel estimation for OFDM," *IEEE Commun. Surveys Tuts.*, vol. 16, no. 4, pp. 1891–1908, 4th Quart., 2014.

[37] Y. S. Cho, J. Kim, and W. Y. Y. C.-G. Kang, *MIMO-OFDM Wireless Communications With MATLAB*. Hoboken, NJ, USA: Wiley, 2010.

[38] J. Zhao, S. K. Ibrahim, D. Rafique, P. Gunning, and A. D. Ellis, "A novel method for precise symbol synchronization in double-side band optical fast OFDM," in *Proc. Opt. Fiber Commun. Conf. Expo. Nat. Fiber Optic Eng. Conf.*, Los Angeles, CA, USA, Mar. 2011, pp. 1–3.

[39] T. M. Schmidl and D. C. Cox, "Robust frequency and timing synchronization for OFDM," *IEEE Trans. Commun.*, vol. 45, no. 12, pp. 1613–1621, Dec. 1997.

[40] T. Xu, S. Mikroulis, J. E. Mitchell, and I. Darwazeh, "Bandwidth compressed waveform for 60-GHz millimeter-wave radio over fiber experiment," *J. Lightw. Technol.*, vol. 34, no. 14, pp. 3458–3465, Jul. 15, 2016.

[41] F. Petenaude and M. L. Moher, "A new symbol timing tracking algorithm for $\pi/2$-BPSK and pi/4-QPSK modulations," in *Proc. IEEE Int. Conf. Commun. Conf. Rec. ICC SUPERCOMM/ICC Discovering New World Commun.*, vol. 3. Chicago, IL, USA, Jun. 1992, pp. 1588–1592.

[42] Aeroflex Test Solutions. *3020 Series RF Signal Generators*. Accessed: May 2017. [Online]. Available: http://ats.aeroflex.com/modular-instrumentation-pxi-products/pxisystems-solutions/modules/3020-series-rf-signal-generators

[43] Aeroflex Test Solutions. *3030 Series PXI RF Digitizers*. Accessed: May 2017. [Online]. Available: http://ats.aeroflex.com/modularinstrumentation-pxi-products/pxi-systems-solutions/modules/3030-series-pxi-rf-digitizers

[44] Aeroflex Test Solutions. *3010/3011 RF Synthesizers*. Accessed: May 2017. [Online]. Available: http://ats.aeroflex.com/modular instrumentation-pxi-products/pxi-systems-solutions/modules/3010-3011-rf-synthesizers

[45] Spirent Communications plc. *VR5 HD Spatial Channel Emulator*. Apr. 2018. [Online]. Available: http://www.spirent.com/Products/VR5

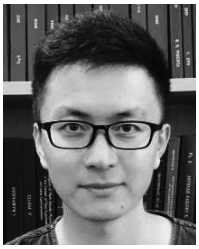

Tongyang Xu (M'18) received the B.Eng. degree in electronic information engineering from Xidian University, Xi'an, China, in 2011, and the M.Sc. degree (with distinction) in telecommunications and Ph.D. degree in electronic and electrical engineering from University College London (UCL), London, U.K., in 2012 and 2017, respectively.

In 2013, he joined the Communications and Information Systems Group, Department of Electronic and Electrical Engineering, UCL. He has authored or co-authored over 25 papers in the areas of wireless and optical communications. He contributed chapters in *Signal Processing for 5G: Algorithms and Implementations* (Wiley, 2016) and *Key Enabling Technologies for 5G Mobile Communications* (Springer, 2016). His current research interests include future fifth-generation communication technology, waveform design, Internet of Things, machine learning, data analysis, real-time testbed design, and antenna design, design and implementation of wireless and optical spectrally efficient communication systems on real-time experimental platforms, power efficient IoT technologies development, machine learning technologies for signal waveform optimization, and precommercialization prototype of an electronically steerable parasitic array radiator transceiver.

Dr. Xu was a recipient of the Faculty of Engineering Sciences Scholarship, UCL in 2013, the nominated investigator of the two successful "Impact Acceleration Discovery to Use" Awards, UCL in 2016 and 2018, and was a co-recipient of the Smart Agriculture Entrepreneurship Grant at Rothamsted Research in 2017.

Izzat Darwazeh (SM'03) received the graduation degree in electrical engineering from the University of Jordan, Amman, Jordan, in 1984 and the M.Sc. and Ph.D. degrees from the University of Manchester, Manchester, U.K., in 1986 and 1991.

He holds the University of London Chair of Communications Engineering and leads the 70-strong Communications and Information Systems Group, Department of Electronic and Electrical Engineering, University College London (UCL). He is also the Director of ICCS, UCL Institute of Communications and Connected Systems. He has authored or co-authored over 250 papers and book chapters in the areas of optical and wireless communications and monolithic microwave integrated circuits and high-speed/frequency circuits. He coedited *Analogue Optical Fibre Communications* (IEE, 1995) and *Elsevier-Newness Book on Electrical Engineering* (Elsevier–Newness, 2008). He co-authored *Linear Circuit Analysis and Modelling* (Elsevier, 2005) and *Microwave Active Circuit Analysis and Design* (Academic, 2015). He currently teaches mobile and wireless communications and circuit design and his current research activities are in ultra high-speed microwave circuits and in wireless and optical communication systems. In 2002, he proposed (with Miguel Rodrigues) the Fast OFDM concept and, in 2003, the SEFDM concept, and has been involved with research on these topics ever since.

Prof. Darwazeh is a Chartered Engineer. He is a Fellow of the IET and the Institute of Telecommunications Professionals FITP.